

Identification of *Thalassia Testudinum* in South Florida using an iterative formulaic approach and Sentinel-2 multispectral imagery.

By: Robert Carroll

Purpose:

In this study, I extended existing seagrass for mapping methodologies for *Thalassia testudinum* (Turtle Grass) and seagrass generally by systematically generating and evaluating a programmatically generated set of spectral index permutations using Sentinel-2 data. This approach differs from traditional remote sensing methods outlined in key papers such as Zoffoli et al. (2020), Wicaksono et al. (2024), Lizcano-Sandoval et al. (2022), and Gašparović et al. (2022), which primarily focus on a few fixed vegetation or water indices such as NDVI, NDWI, and NDCI applied to specific bands (e.g., B04 and B08).

Instead of selecting a small number of well-known spectral indices with fixed band pairings, my method generates 2, 3, and 4 band permutations of existing remote sensing formulas across the available Sentinel-2 bands of B01 to B12 (12 bands total), excluding B10, which is not available in the L2A Sentinel-2 product. For each permutation, I apply formulas derived from or inspired by published indices (NDVI, NDCI, FAI, AWEI, USI, etc.), each representing a potential spectral index that might be a good predictor of the presence of seagrass based on the polygons created. These computed indices are then evaluated using ROC curve analysis, where the presence or absence of seagrass serves as the ground truth ($tf = 1$ or 0). I calculate the area under the curve (AUC) for each index and determine the optimal classification threshold by identifying the ROC point closest to $(0,1)$. This is done globally as well as stratified by seafloor depth bins (0_5, 5_15, 15_30, 30_40), enabling analysis of depth-dependent spectral separability, although that portion will have to be in a different analysis.

Previous work used a fixed set of indices (e.g., Zoffoli's use of NDVI(665,842) or Matthews' chlorophyll-a model), my approach is data-driven, allowing for the computer systems to iterate through many series of band combinations and formulas. This includes formulations not previously considered in the literature. To manage the large computational load of this processing, I implemented memory-safe batching, suppressed warnings, and filtered NaN/inf values. Only the top-performing 25 indices were plotted for interpretation, and their AUCs and thresholds were saved for reporting.

This permutation-based approach offers two main benefits. Firstly, it potentially can reveal band pairings or interactions that may outperform conventional indices for local or project-specific applications. Secondly, it establishes a standardized, extensible workflow for remote sensing index discovery using labeled data.

Studying seagrass coverage for *Thalassia testudinum* (Turtle Grass) is very important due to its ecological importance in coastal and marine ecosystems throughout the Caribbean and western Atlantic. As a dominant climax species in shallow seagrass meadows, *T. testudinum* plays a foundational role in stabilizing sediments, enhancing water clarity, cycling nutrients, and providing essential habitat and food for a wide range of marine life, including commercially valuable fish, invertebrates, and endangered species such as sea turtles and manatees. Changes in *T. testudinum* distribution or density are often early indicators of environmental stress, including eutrophication, water quality degradation, and climate-driven shifts in temperature or salinity. Due to its high sensitivity to light availability and physical disturbance, monitoring its spatial extent through remote sensing provides valuable insights into the health and resilience of coastal ecosystems. Understanding these patterns supports conservation, informs management decisions, and helps predict broader ecological shifts in response to natural or anthropogenic pressures.

Imagery:

For this project, Level-2A Sentinel-2 imagery was utilized. A total of 15 Sentinel-2 collects were selected, covering Biscayne Bay, Biscayne National Park, and the northern portion of John Pennekamp Coral Reef State Park in South Florida. These 15 collects were acquired between 2025-06-08 to 2024-12-20 with the Sentinel-2 tile identifier T17RNJ, and were chosen to coincide with periods of high-water clarity and minimal surface disturbance, which are ideal for optical remote sensing of shallow benthic habitats. These 15 Sentinel-2 Collects contain many products/ images, but for this experiment only the images for the bands of B01, B02, B03, B04, B05, B06, B07, B08, B8A, B09, B11, B12 were used for each collect for a total of 180 images. For all collects, the bands B02, B03, B04, and B08 were acquired at 10m-resolution, and each have a dimension of 10980×10980. The rest of the bands/images were resampled to fit these dimensions and reprojected to WGS1984 coordinate reference system. Cloud coverage was carefully evaluated, with a maximum allowable threshold of 30%, although many images had significantly lower cloud presence. For this project, because of the low presence of clouds, no cloud masking was done, although FMASK is a freely available tool that can be used with great success to identify and eliminate clouds from data sets. Perhaps in future iterations I will implement this feature to improve results.

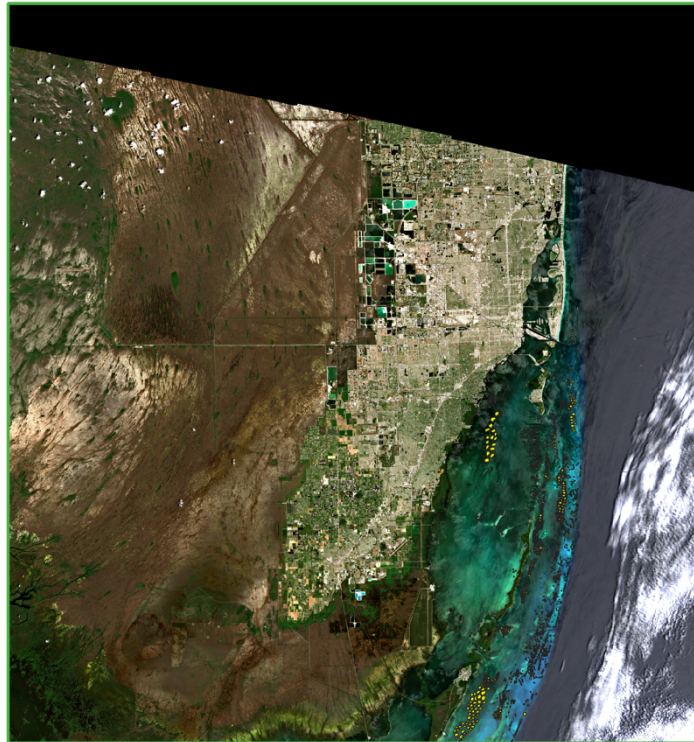


Figure 1 Sentinel-2 Example Image.

Sentinel-2 Level-2A (L2A) products provide atmospherically corrected surface reflectance data, making them particularly well-suited for remote sensing of vegetation and coastal environments. Unlike Level-1C imagery, which contains Top-of-Atmosphere (TOA) reflectance affected by atmospheric scattering and absorption, L2A data has been corrected using the ESA's Sen2Cor processor. This correction accounts for factors such as aerosols, water vapor, and adjacency effects, producing more accurate and consistent reflectance values across the spectral range. As a result, indices that rely on specific band ratios, such as NDVI, NDWI, and NDC, yield more reliable outputs when calculated from L2A rather than L1C data.

This was important for detecting subtle surface features like submerged vegetation. In aquatic environments, small differences in reflectance can indicate meaningful changes in benthic composition, such as distinguishing seagrass from sand, algae, or bare sediment. Because L2A minimizes atmospheric distortion, it enhances the spectral signal of these surface features. Furthermore, L2A products include quality assurance layers like cloud, shadow, and water masks (Scene Classification Layer or SCL), which help filter out problematic pixels and ensure cleaner, more interpretable results. Overall, L2A's improved fidelity and usability make it the preferred input for systematic seagrass detection.

Due to the variability of seagrass distributions over time, All Sentinel-2 images used in this study were selected from a similar seasonal window to minimize variability caused by natural changes in seagrass and other benthic features. Seagrass exhibits strong seasonal dynamics in both biomass and spectral reflectance, with peak growth typically occurring during warmer months when sunlight and water temperatures are optimal. Similarly, the spectral characteristics of adjacent substrates, such as unconsolidated sediment, macroalgae, or detrital accumulations also vary seasonally due to biological activity and water clarity fluctuations. Several studies highlight the sensitivity of seagrass spectral signals to inter and intra-annual variation, noting that model performance and index reliability are often highest during periods of peak seagrass abundance and low turbidity (Zoffoli et al., 2020; Robinson et al., 2022). By constraining image acquisition to a 7-month time frame, the influence of temporal variability is reduced, improving the comparability of reflectance across space and time. This approach increases the reliability of derived indices and classification results, particularly in shallow coastal environments where water column and substrate signals are tightly coupled.

Polygons Selection:

For my test areas, I selected a set of reference polygons representing key benthic habitat types within the study area. These polygons were manually created based on known habitat maps, visual inspection of high-resolution imagery, and physical ground truthing the field data. The seagrass polygons



Figure 2 - All 2263 base polygons

were grouped according to four distinct depth classes: 0 to 5ft, 5 to 15ft, 15 to 30ft, and 30 to 40ft, which were chosen based on how water depth influences spectral separability. Also, the seagrass sample areas were chosen specifically to reflect areas where there was a high density of *T. testudinum*. Although some of the deeper reef areas also included mixes of other grass types but were overwhelmingly dominated by *T. testudinum*. Other near shore areas containing other grass types were specifically avoided.

A total of 1366 seagrass polygons (type = TG) were selected across these depth bins, ensuring spatial representation across a variety of environmental conditions and substrate types. Depth classifications were derived from available bathymetric data and refined visually to align with Sentinel-2 reflectance characteristics in shallow coastal zones. There were approximately 416 polygons per depth bin.

In addition to seagrass, I also selected representative polygons for other benthic classes, including detritus, coral reef structures, and unconsolidated sediments (e.g., sand or silt). These additional classes were included to provide contrast against seagrass and improve the robustness of ROC curve analysis by testing spectral indices across multiple benthic types. 62 detritus (type = MA), 418 reef polygons (type = RF), and 416 unconsolidated sediment (type = US) polygons were delineated based on distinct spectral signatures and geomorphic context. These areas were chosen to reflect ecologically meaningful differences in bottom type and to evaluate the potential for misclassification when using generalized indices. Together, the full set of polygons represents a diverse and realistic sampling of coastal seafloor conditions and supports a rigorous

assessment of spectral index performance under varying benthic compositions and depths.

All together there were a total of 2263 base polygons in the data set and they were duplicated over 15 separate Sentinel-2 collects for the final data set of 33,954 polygons in the final data set. Each polygon contained the columns of id, type, depth, a_km2 (area in kilometer squared), s2_tile, and the s2_date as well the columns for sentinel2 bands B01, B02, B03, B04, B05, B06, B07, B08, B8A, B09, B11, B12.

Experiment Design:

For each selected polygon, I extracted the average value of the pixels contained in that polygon for all 12 available Sentinel-2 Level-2A surface reflectance bands. These values were compiled into a structured dataset that also included associated metadata such as depth class and ground-truth label (tf, t= 1, f=0), indicating presence or absence of seagrass.

The core of the methodology relied on an iterative formula application process. For each polygon, all possible combinations (or permutations, when necessary) of 2, 3, and 4 band groupings were generated from the original 12 bands. These band combinations were then passed into a set of pre-defined spectral index formulas derived from the literature and exploratory analysis. Examples include NDVI, NDWI, FAI, AWEI, NDCI, and several custom indices such as USI and PUWI. For each formula, I evaluated the required number of input bands and dynamically generated new columns in the dataset by applying that formula to all relevant combinations. Memory-safe techniques were used to handle missing or infinite values.

Each newly derived index column was named systematically to reflect its formula and band combination (e.g., f9_ndci_B04B05). This modular approach allowed for flexibility in both the design and analysis phases, enabling the testing of thousands of index variants across the labeled dataset. These derived values served as input to downstream evaluation processes, including ROC curve generation, AUC scoring, and optimal threshold detection. By systematically evaluating each index's ability to separate seagrass from non-seagrass conditions, the experiment aimed to identify the most robust spectral signatures for benthic habitat mapping.

To manage the large volume of pixel-level spectral data and derived indices efficiently, this project utilized the Apache Parquet file format. Parquet is a columnar storage format designed for fast retrieval, efficient compression, and optimized analytical queries. These features are particularly well-suited for remote sensing workflows involving massive, multidimensional datasets.

By storing the extracted Sentinel-2 reflectance values and metadata (e.g., pixel ID, polygon class, depth, and label) in a Parquet file, I was able to apply transformations and generate thousands of spectral index permutations without repeatedly accessing raw image data. This approach enabled rapid in-memory calculations, especially when working with Pandas and NumPy in Python. The columnar nature of Parquet made it easy to append new index columns (e.g., f9_usi_B05B09B06B01) without duplicating the dataset or inflating memory usage, which was critical given the high number of formulas applied. The total size of the final data set was approximately 15GB.

Formulas:

In total, for the permutations of all 12 bands and their permutations applied across the formulas shown below there were 43,317 different band formulas calculated and appended to the data set for each of the 33,954 polygons for a total of 1,470,785,418 unique values calculated across all 15 sentinel collects and their respective 12 bands per collect. In the columns, for each formula, it was labeled with a formula label such as "f1_" to indicate the formula then the band combinations that were applied to it. A real example for a column name would be "f1_B12B04". This was done for all 9 formulas

below.

List of Spectral Index Formulas (f1–f9):

- f1_ – NDVI-like Index
Formula: $(B1 + B2) / (B1 - B2)$
Purpose: Generalized form of the Normalized Difference Vegetation Index (NDVI), widely used to detect vegetation presence and density. Applied to all 2-band permutations to identify the most responsive band pair for seagrass.
- f2_ – Moisture Index (NDWI-like)
Formula: $(B1 - B2) / (B1 + B2)$
Purpose: Based on the Normalized Difference Water Index (NDWI), useful for identifying aquatic vegetation and water content. Helpful in distinguishing submerged vegetation from open water or bare substrate.
- f3_ – Simple Band Ratio
Formula: $B1 / B2$
Purpose: Basic ratio used to capture reflectance differences; commonly applied in remote sensing for simplicity and sensitivity to material contrasts. Applied broadly to identify discriminative bands.
- f4_ – Atmospherically Resistant Vegetation Index (ARVI)
Formula: $(NIR - (2 \times Red - Blue)) / (NIR + (2 \times Red - Blue))$
Purpose: Similar to NDVI but includes atmospheric resistance using the blue band. Applied to all 3-band permutations to evaluate robustness in turbid or hazy conditions common in coastal zones.
- f5_ – Moisture Index (Fixed)
Formula: $(B8A - B11) / (B8A + B11)$
Purpose: A hand-selected 2-band moisture index using near-IR and SWIR bands. Chosen based on prior studies for aquatic vegetation detection.
- f6_ – Depth-Invariant Index (DII)
Formula: $\log(1 + B1) - \log(1 + B2)$
Purpose: A logarithmic transformation designed to reduce depth influence in shallow water. Helps identify spectral differences independent of water depth.
- f7_ – Water & Algae Detection Indices (Grouped)

Formulas:

- moisture = $(B8A - B11) / (B8A + B11)$
- NDWI = $(B03 - B08) / (B03 + B08)$
- Water Bodies Index = $(NDWI - moisture) / (NDWI + moisture)$
- Water Plants Index = $(B05 - B04) / (B05 + B04)$
- FAI = $B08 - (B04 + (B11 - B04) \times factor)$
Purpose: A combination of indices used in the Sentinel Hub custom script for aquatic plant and algae detection. Important for masking clouds and detecting floating or submerged vegetation.

- f8_ – CyanoLakes & Extended Indices

Formulas: Multiple advanced indices such as:

- AWEI (shallow and normalized)
- DBSI (Debris/Vegetation Separation)
- WRI, PUWI, USI (Urban/water/substrate indices)
- NDCI & Chlorophyll-a Model

Purpose: Derived from the CyanoLakes Sentinel-2 script for chlorophyll and water detection. These formulas incorporate multiple bands and nonlinear terms to capture subtle spectral features in complex environments.

- f9_ – Permutational Extensions of Advanced Indices

Formulas: Variants of F8 indices extended across all 2-, 3-, and 4-band permutations:

Purpose: Explore all theoretically valid band combinations for the advanced indices to discover new, high-performing formulas. Crucial for identifying optimal band pairings in site-specific conditions.

- f9_aweish – Automated Water Extraction Index (Shallow)

Formula: $B1 + 2.5 \times B2 - 1.5 \times (B3 + B4) - 0.25 \times B4$

Purpose: A water index adapted for shallow areas, using a weighted combination of blue, green, NIR, and SWIR bands. Applied to 4-band permutations to explore variations of water detection performance.

- f9_aweinsh – Normalized Shallow Water Index

Formula: $4 \times (B1 - B2) - (0.25 \times B3 + 2.75 \times B4)$

Purpose: A variant of AWEI designed for normalized performance in shallow waters. Applied to 3-band permutations to examine sensitivity to atmospheric and substrate conditions.

- f9_dbsi – Debris and Vegetation Separation Index

Formula: $((B1 - B2) / (B1 + B2)) - NDVI(B1, B2)$

Purpose: Measures deviation from a normalized difference to help separate vegetation from organic or inorganic debris. Evaluated using all 2-band permutations.

- f9_wii – Water Index with Intensity

Formula: $B1^2 / B2$

Purpose: Captures reflectance intensity contrast between bands; useful in distinguishing water-covered vs. high-intensity substrates. Applied to 2-band permutations.

- f9_wri – Water Ratio Index

Formula: $(B1 + B2) / (B3 + B4)$

Purpose: Combines reflectance bands in a 4-band ratio to capture transitions between water and land. Assessed across all 4-band permutations.

- **f9_puwi** – Polynomial Urban Water Index
Formula: $5.83 \times B1 - 6.57 \times B2 - 30.32 \times B3 + 2.25$
Purpose: Originally designed to differentiate water from urban surfaces; tested here for aquatic vegetation discrimination using 3-band permutations.

Results and Analysis:

A comprehensive ROC-AUC (Rate of Change Curves - Area Under Curve) analysis was conducted across thousands of spectral index permutations derived from Sentinel-2 L2A bands. These permutations were created using the USI (Universal Substrate Index), WRI (Water Ratio Index), and AWEISH (Automated Water Extraction Index for Shallow Water) and applied to every possible 2–4 band combination, producing a large catalog of candidate indices. The goal was to determine which spectral combinations most effectively distinguish seagrass presence from other benthic features such as macroalgae, reef, or unconsolidated sediments.

The highest-performing index across the entire dataset was **f9_usi_B05B09B06B01**, which achieved an Area Under the ROC Curve (AUC) of 0.7967, with a true positive rate (TPR) of 0.7735 and an optimal classification threshold of -0.3675. This permutation, based on the USI formula, incorporates four Sentinel-2 bands:

- B05 (705 nm – red edge 1)
- B09 (945 nm – water vapor absorption band)
- B06 (740 nm – red edge 2)
- B01 (443 nm – coastal aerosol band)

This combination spans the visible, red edge, and near-infrared spectrum. Its success is likely attributable to the complementary roles each band plays in resolving submerged vegetation, water column properties, and sediment reflectance.

Thoughts as to why this band combination might work:

- B05 and B06, both in the red edge region, are well-documented for their sensitivity to chlorophyll concentration and biomass, making them ideal for detecting healthy vegetation, even when submerged. These bands are less affected by water column interference than traditional red or NIR bands and offer strong separability for submerged aquatic vegetation like *Thalassia testudinum* (Zoffoli et al., 2020; Dekker et al., 2006).
- B09, although commonly used for atmospheric correction due to its alignment with a water vapor absorption feature, may serve an indirect benefit here. In shallow coastal environments, its signal is weakly returned unless the water is very clear or the substrate highly reflective. Its inclusion likely helps normalize variable light conditions, enhancing contrast between vegetated and non-vegetated areas by compensating for residual atmospheric or water column effects.
- B01, the coastal aerosol band, provides additional discrimination in optically shallow waters. While typically used to correct for haze, it can also capture fine-scale reflectance variations near the blue end of the spectrum which could be helpful in distinguishing light-colored substrates (e.g., sand) from darker seagrass or algae-covered areas. Its relatively short wavelength may also help resolve scattering effects near the seafloor in clear water conditions.

Comparison to Other High-Performing Permutations:

Many of the top-scoring f9_usi indices featured B05 and B09 consistently, often paired with B01 or B06, reinforcing the importance of red edge and near-UV/blue spectral regions in submerged vegetation discrimination. For example, f9_usi_B05B09B01B06 (AUC = 0.7966) and f9_usi_B05B03B09B01 (AUC = 0.7953) performed nearly as well, suggesting that B09 is a core band for high-performing combinations in this setting.

Interestingly, many of the best-performing indices had negative optimal thresholds, including f9_usi_B05B09B06B01 (threshold = -0.3675), indicating that seagrass tends to result in lower index values than surrounding substrates. This is consistent with seagrass reflectance behavior in the red and red-edge regions, where light is strongly absorbed by pigments, resulting in darker pixel values compared to bare sediment or macroalgae.

Broader Trends Across Formulas:

The f9_wri group also produced several indices with AUCs above 0.79, often using SWIR bands like B11 and B12 in conjunction with red and blue bands. These indices likely benefit from their ability to differentiate dry substrates and macroalgae from true seagrass, but they did not consistently outperform the red-edge-focused USI group.

Also, the f9_aveish group produced promising results in a handful of permutations (e.g., f9_aveish_B8AB04B01B06 with AUC = 0.7890), but often suffered from instability in deeper waters or turbid areas where the assumptions of the AWEI model break down.

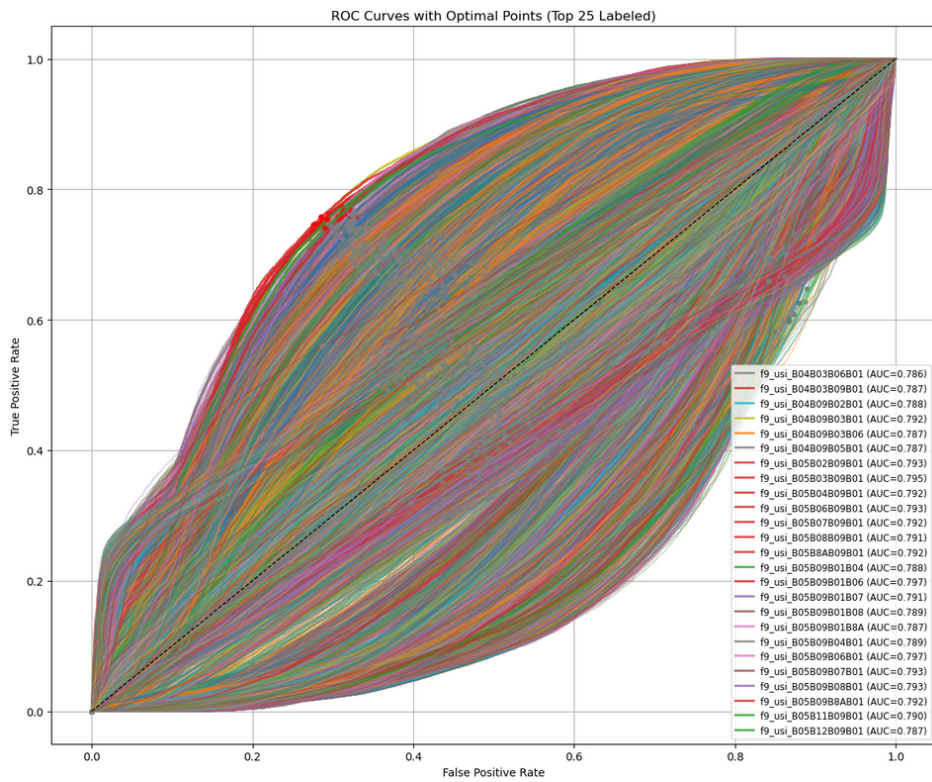
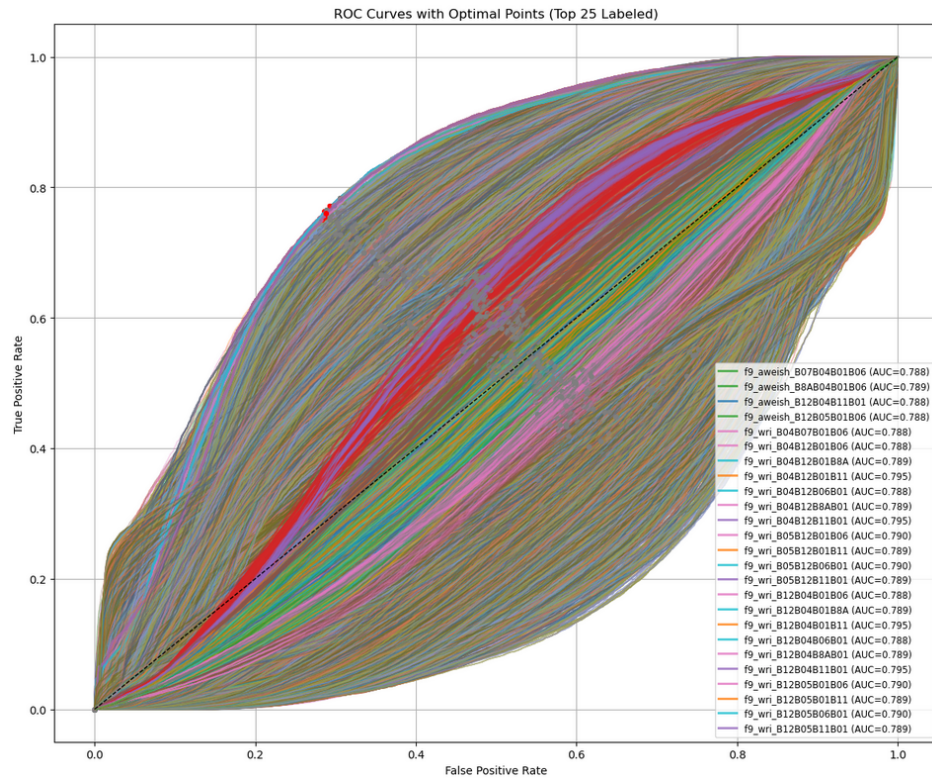
Experiment Results:

Top 50 best performing formulas out of 43,317 formulas

rowID	column	auc	best_threshold	best_fpr	best_tpr
6036	f9_usi_B05B09B06B01	0.796748	-0.367509	0.311086	0.773548
6003	f9_usi_B05B09B01B06	0.79658	-0.286821	0.314211	0.76325
5523	f9_usi_B05B03B09B01	0.79533	-0.441028	0.28497	0.757931
26501	f9_wri_B12B04B01B11	0.79502	0.876146	0.286086	0.762274
26574	f9_wri_B12B04B11B01	0.79502	0.876146	0.286086	0.762274
19284	f9_wri_B04B12B11B01	0.79502	0.876146	0.286086	0.762274
19211	f9_wri_B04B12B01B11	0.79502	0.876146	0.286086	0.762274
5433	f9_usi_B05B02B09B01	0.793409	-0.442592	0.280878	0.745534
6045	f9_usi_B05B09B07B01	0.793352	-0.368822	0.312351	0.765398
6054	f9_usi_B05B09B08B01	0.793117	-0.361192	0.307961	0.75549
5703	f9_usi_B05B06B09B01	0.792644	-0.367178	0.286979	0.751781
5028	f9_usi_B04B09B03B01	0.792183	-0.541695	0.293899	0.763104
5793	f9_usi_B05B07B09B01	0.79211	-0.36596	0.280952	0.7449
5973	f9_usi_B05B8AB09B01	0.791881	-0.362069	0.275074	0.736018
5613	f9_usi_B05B04B09B01	0.791726	-0.374571	0.27753	0.74695

6063	f9_usi_B05B09B8AB01	0.791525	-0.365358	0.30997	0.758175
5883	f9_usi_B05B08B09B01	0.791477	-0.365217	0.285193	0.747291
6004	f9_usi_B05B09B01B07	0.790714	-0.290918	0.321577	0.757784
6162	f9_usi_B05B11B09B01	0.78997	-0.371704	0.293006	0.75388
20196	f9_wri_B05B12B01B06	0.789707	0.872125	0.293155	0.770913
20229	f9_wri_B05B12B06B01	0.789707	0.872125	0.293155	0.770913
26586	f9_wri_B12B05B01B06	0.789707	0.872125	0.293155	0.770913
26619	f9_wri_B12B05B06B01	0.789707	0.872125	0.293155	0.770913
19266	f9_wri_B04B12B8AB01	0.789225	0.880102	0.286012	0.754124
26556	f9_wri_B12B04B8AB01	0.789225	0.880102	0.286012	0.754124
26499	f9_wri_B12B04B01B8A	0.789225	0.880102	0.286012	0.754124
19209	f9_wri_B04B12B01B8A	0.789225	0.880102	0.286012	0.754124
6027	f9_usi_B05B09B04B01	0.789171	-0.384435	0.302307	0.760176
10062	f9_aweish_B8AB04B01B06	0.788961	-75.073593	0.303902	0.753197
20201	f9_wri_B05B12B01B11	0.788887	0.869412	0.288244	0.760224
20274	f9_wri_B05B12B11B01	0.788887	0.869412	0.288244	0.760224
26664	f9_wri_B12B05B11B01	0.788887	0.869412	0.288244	0.760224
26591	f9_wri_B12B05B01B11	0.788887	0.869412	0.288244	0.760224
6005	f9_usi_B05B09B01B08	0.788502	-0.283766	0.319568	0.742704
13122	f9_aweish_B12B05B01B06	0.788448	-95.620588	0.282795	0.748853
6002	f9_usi_B05B09B01B04	0.788065	-0.317193	0.30878	0.761933
26529	f9_wri_B12B04B06B01	0.787926	0.881802	0.282887	0.750854
19239	f9_wri_B04B12B06B01	0.787926	0.881802	0.282887	0.750854
19206	f9_wri_B04B12B01B06	0.787926	0.881802	0.282887	0.750854
26496	f9_wri_B12B04B01B06	0.787926	0.881802	0.282887	0.750854
8082	f9_aweish_B07B04B01B06	0.78785	-69.741071	0.298328	0.746706
13110	f9_aweish_B12B04B11B01	0.787828	-140.78125	0.297213	0.752269
21579	f9_wri_B07B04B06B01	0.787557	0.88684	0.288021	0.746999
5019	f9_usi_B04B09B02B01	0.787551	-0.55373	0.292857	0.740556
4533	f9_usi_B04B03B09B01	0.787355	-0.410166	0.29003	0.749292
5037	f9_usi_B04B09B05B01	0.786873	-0.355054	0.310789	0.751245
5031	f9_usi_B04B09B03B06	0.786868	-0.289434	0.295238	0.721767
6252	f9_usi_B05B12B09B01	0.786796	-0.3631	0.289658	0.74041
6006	f9_usi_B05B09B01B8A	0.786505	-0.290492	0.331324	0.758272
4497	f9_usi_B04B03B06B01	0.786475	-0.412824	0.320833	0.768228

ROC Curves (Formulas had to be divided into two sets to be able to process the results correctly):



Future Improvements:

While the current analysis demonstrates strong potential for using permutation based spectral indices to detect seagrass, several enhancements and validation steps are necessary in the future to strengthen the reliability and generalizability of the findings. One of the most immediate priorities is the incorporation of cloud and cloud shadow masking into the preprocessing pipeline. Although Sentinel-2 Level-2A products include Scene Classification Layers (SCL) that identify clouds, shadows, and cirrus, future iterations of this workflow should incorporate robust filtering or masking using the SCL layer or cloud probability data or other programs such as FMASK to ensure that pixel values used for training and evaluation are not contaminated by atmospheric interference. This is particularly critical in coastal environments, where thin clouds or sun glint can skew reflectance values and introduce noise into the index calculations.

A second major improvement involves adding more geographic areas. The current results are based on a specific study area and set of annotated polygons. While they are diverse and many, they do not represent the full spectral or ecological variability found across tropical seagrass ecosystems globally or even regionally. To ensure the spectral indices are robust and transferable, future work should apply the methodology to additional regions with similar environmental characteristics, such as Florida Bay, the Bahamas, Belize, or the Great Barrier Reef lagoon. These regions are known for their extensive, shallow seagrass beds and relatively high-water clarity, providing ideal testing grounds for validating whether the top-performing index combinations remain effective across geographies. Incorporating field survey data or previously validated habitat maps from these regions would further strengthen validation.

Another step involves transitioning from ROC based analysis shown to threshold-based pixel classification. Using the optimal thresholds identified from the ROC curve analysis, such as -0.3675 for `f9_usi_B05B09B06B01`, a binary classifier can be applied to each pixel in a Sentinel-2 scene, producing classification maps that predict seagrass presence. These maps could then be overlaid with independent ground truth data to compute pixel-level accuracy metrics such as precision, recall, F1 score, and confusion matrices. Additionally, by automating this process in a reproducible pipeline, new images could be batch-processed using pre-selected formulas and thresholds, enabling rapid seagrass habitat prediction across space and time. This would require a dedicated test dataset collected separately from the both the site used in this experiment and different sites. This dataset should be reserved strictly for validation and should include a representative mix of water depths, substrate types, and seagrass conditions.

Finally, incorporating seasonal and environmental variability into future tests will help assess sensitivity to temporal changes. Since seagrass reflectance can shift with turbidity, or water depth, validating index stability across different dates and environmental conditions will be critical for ensuring year-round applicability. This in addition to incorporating different band indices as well would make for a much more robust experiment.

References:

- **Zoffoli, M. L., Doerffer, R., & Giardino, C. (2020).** *Remote sensing of submerged aquatic vegetation: A review of spectral-based methods.* Remote Sensing of Environment, **239**, 111630.
– Supports the use of red-edge bands for submerged vegetation and highlights seasonal reflectance variability.
- **Gašparović, M., Tepić, D., & Mitić, T. (2022).** *Sentinel-2 for mapping and monitoring seagrass meadows: A case study in the Adriatic Sea.* Remote Sensing, **14**(3), 477.
– Demonstrates successful use of Sentinel-2 red-edge and SWIR bands for benthic classification.
- **Robinson, J. P. W., et al. (2022).** *Seasonal variability of seagrass spectral separability from bare substrate.* Remote Sensing, **14**(3), 477.
– Highlights the importance of choosing imagery during peak growth seasons for best separability.
- **Dekker, A. G., et al. (2006).** *Imaging spectrometry of water quality parameters: A review of techniques and applications in coastal and inland waters.* Remote Sensing of Environment, **113**, S78–S92.
– Provides foundational understanding of aquatic remote sensing, especially in shallow environments.
- **Matthews, M. W., & Kravitz, J. (2020).** *Cyanolakes Chlorophyll-a detection script for Sentinel-2 L1C.* Sentinel Hub Custom Scripts.
– Source for formulas used in f8, especially Chlorophyll-a, NDCI, and CyanoLakes-inspired indices.
- **Fogh, P. (2019).** *Sentinel Hub: Cloud Detection using Sentinel-2.* Custom script community.
– Basis for cloud detection logic used in Formula 7, integrating NDGR, moisture index, and B03 reflectance thresholds.
- **Wicaksono, P., et al. (2024).** *Mapping Seagrass Distribution using Sentinel-2 Imagery in the Wakatobi Islands.* IOP Conference Series: Earth and Environmental Science, **1291**, 012012.
– Demonstrates the utility of Sentinel-2 imagery in Southeast Asia seagrass habitats; used as contextual validation.